

Fast Simulation of Mitral Annuloplasty for Surgical Planning

Neil A. Tenenholtz¹, Peter E. Hammer^{1,2}, Assunta Fabozzo^{2,3}, Eric N. Feins²,
Pedro J. del Nido², and Robert D. Howe¹

¹ Harvard School of Engineering and Applied Sciences, Cambridge, MA, USA

² Department of Cardiac Surgery, Children's Hospital, Boston, MA, USA

³ Division of Cardiac Surgery, University of Padova, Padova, Italy

Abstract. Mitral valve repair is a complex procedure that requires the ability to predict closed valve shape through the examination of an unpressurized, flaccid valve. These procedures typically include the remodeling of the mitral annulus through the insertion of an annuloplasty ring. While simulations could facilitate the planning of the procedure, traditional finite-element models of mitral annuloplasty are too slow to be clinically feasible and have never been validated in tissue. This work presents a fast method for simulating valve closure post-annuloplasty using a mass-spring tissue model and subject-specific valve geometry. Closed valve shape is predicted in less than one second. The results are validated by implanting an annuloplasty ring in an excised porcine heart and comparing simulated to imaged results. Results indicate that not only can mitral annuloplasty be simulated quickly, but also with sub-millimeter accuracy.

1 Introduction

A competent mitral valve ensures the one-way flow of oxygenated blood from the left atrium to the left ventricle. However, many pathologies damage the valve anatomy producing undesired backflow, or regurgitation, decreasing cardiac efficiency and potentially leading to heart failure if left untreated. Valve repair, the surgical modification of the native valve tissue, is the preferred method of treatment as it produces the best long-term survival [1, 2]. Key to the procedure is the annuloplasty, the insertion of a prefabricated ring to reshape the mitral annulus, which is employed in over 97% of cases [3]. However, treating the valve with an annuloplasty alone and excluding other common repair techniques has been demonstrated to increase the risk of reoperation and decrease long-term survivability [4]. Therefore, it is crucial that the surgeon understand how the ring affects closed valve shape so that these other techniques can be used to effectively complement the annuloplasty and restore valve competency.

Prior research has focused on complex finite element models to predict closed-valve shape post-annuloplasty [5–7]. However, such work has been plagued by two primary weaknesses in the context of surgical planning. While these models can produce highly accurate results, finite element models of the mitral valve

have traditionally been computationally expensive with simulation times of valve closure on the order of hours if not days [8]. The accuracy of these models can produce great insights into valve function, but their simulation time makes them infeasible in a clinical setting. In addition, methods for segmenting the complete valve and subvalvular apparatus in-vivo have yet to be developed with segmentation of the fine chordae tendineae proving to be challenging. As a result, simulations of mitral annuloplasty have never been validated outside of a computer. In contrast, others have analyzed in-vivo the effects of mitral annuloplasty on annular and leaflet strain but did so through the direct observation of tantalum markers and did not predict closed valve shape [9, 10].

To address these deficiencies, we have developed a new method to simulate and validate mitral annuloplasty. A freshly excised porcine heart is imaged using microCT to generate a subject-specific valve model. The model is simulated to closure in less than one second both before and after valve annuloplasty using a mass-spring tissue model, first proposed in [11]. A second microCT image is then taken after ring insertion and compared to the simulated results, thus producing the first validated simulation of mitral valve annuloplasty.

2 Methods and Materials

2.1 Valve Model Generation

While methods have been developed for extracting leaflet and annular geometry from clinical 3D ultrasound volumes [12, 13], a complete valve model including the subvalvular apparatus has yet to be developed. Therefore, to better isolate simulation error from imaging and geometric modeling error, high resolution computed tomography (MicroCAT II, Siemens) was selected for its increased resolution (100 μm isotropic voxel size) and improved noise characteristics (Figure 1(a)).

To enable the use of microCT, the hearts used in this experiment were freshly excised from 25-30 kg Yorkshire pigs. Valve closure was induced by pressurizing the left ventricle with air delivered via tubing introduced through the aorta. Pressure was precisely controlled using a regulator and pressure transducer. Transvalvular pressure was set between 70 and 85 mmHg, depending on the load the valve could withstand without regurgitation. To prevent unintended leakage, we also ligated the coronary arteries and sealed them using cyanoacrylate. Images were taken of the unpressurized and pressurized valve to generate the valve model.

Using custom software, the mitral valve and subvalvular apparatus were segmented from the volumetric images. Unstressed leaflet geometry and chordal attachment points were acquired from the unpressurized valve. A smooth mesh of 600-700 faces was fit to the unstressed leaflet geometry using a combination of downsampling and edge relaxation techniques. Pressurized annular shape, displaced papillary locations, and the lengths of the individual chordae tendineae were determined using the image of the pressurized valve.

2.2 Simulation of Valve Closure

Finite element models are the standard for mechanical membrane simulations. However, they are also an order of magnitude slower than mass-spring approximations and provide a minimal improvement in accuracy in the context of valve simulation [14]. To avoid these increased computational costs, an isotropic membrane mass-spring tissue model was used to simulate valve mechanics. Springs were assigned a bilinear force law to approximate a more complex Fung-elastic constitutive law. Piecewise-continuous, the bilinear curve contains a highly distensible region below a critical strain of 25% and a significantly stiffer post-transition region with stiffness values selected to best match the biaxial testing data found in literature [15, 16]. Resting spring lengths were determined using edge lengths from the unpressurized mesh. Leaflet tissue was assigned a uniform 1mm thickness.

Chordae tendineae were treated as linear elastic cylindrical rods with a 1mm diameter supporting only uniaxial tension. Since the chordae are significantly stiffer than leaflet tissue, their resting length was taken to be that observed in the closed valve state. Dirichlet boundary conditions were provided by the fibrous mitral annulus and papillary muscles.

To induce valve closure and predict closed valve shape, a static load of peak-systolic pressure was introduced¹. While such a load does not accurately represent systole in-vivo, it does approximate a common intra-operative test used for assessing valve competence. In addition, since the load applied is the maximum the valve will face during the cardiac cycle, we are testing the peak mechanical challenge and therefore the greatest likelihood of regurgitation. This approximation avoids the need for computing fluid-structure interactions, allowing for significantly faster, clinically feasible simulations. The resulting forces are applied in the direction of the face normals and divided equally among each of the faces' three vertices.

Collision handling is implemented in two phases. First, broadphase collision detection is performed and the list of potential collisions is updated using a cache-friendly sweep and prune algorithm. Candidate pairs are then evaluated on a pairwise basis. A nonlinear, penalty-based restoring force is used to prevent inter-penetration.

2.3 Valve Annuloplasty

A custom annuloplasty ring was designed and constructed using a 3D printer, mimicking the shape and function of standard clinical annuloplasty rings but constructed to minimize imaging artifacts. As seen in Figure 1(b), the ring was designed with a series of holes through which sutures could be passed. Then, as shown in Figure 1(c), the ring was surgically implanted into the porcine hearts by a trained cardiac surgeon. Valve closure was again induced using air introduced through the aorta. The closed valve was imaged using computed tomography and segmented (Figure 1(d)).

¹ The actual load was determined by the transvalvular pressure used during imaging.

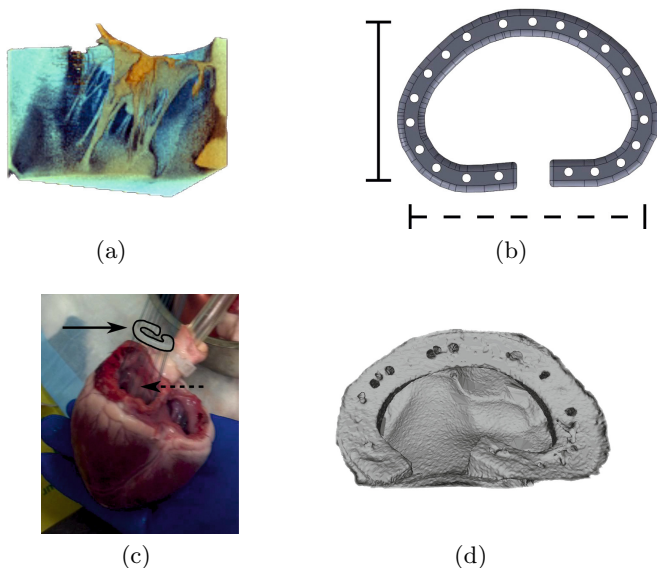


Fig. 1. (a) MicroCT is used to image valve geometry allowing for the chordal structure to be reconstructed. (b) A 3D-printed split annuloplasty ring was developed with anteroposterior (solid marker) and transverse (dashed marker) dimensions mimicking commercially available rings. (c) The ring (solid arrow, artificially outlined due to its translucency) is sutured into the mitral valve (dashed arrow) of an excised porcine heart by a trained cardiac surgeon. (d) The ring is clearly visible in the resulting microCT image.

To simulate an annuloplasty, the ring was aligned to the mitral valve model using the image of the valve after ring insertion. The vertices of the valve model located on the mitral annulus were then warped to the nearest point on the ring. The valve was simulated to closure with its new annular geometry. The simulated results were then compared to the segmented image.

3 Results

Two porcine hearts were segmented, and the mitral valve and its subvalvular apparatus were isolated. Leaflet geometry was represented by meshes of 639 and 674 faces respectively. Chordal geometry varied notably in the two models. While the two hearts demonstrated similar counts of papillary-chordal junctions (21 and 25 respectively²), the branching structure varied widely.

Using a laptop with an Intel Core i5 processor and 8 GB of memory, four simulations were run till closure (pre-annuloplasty and post-annuloplasty models for each of the two hearts). In each instance, simulation required less than 1

² Multiple chordae branching from a single papillary head were not combined.

second to complete. Table 1 shows the RMS and maximum error for each of the four cases, where error is defined to be the distance from the simulated valve to the segmented imaged valve. Figure 2 maps this error onto the simulated valve.

Table 1. Error (in mm) across the four valve simulations. Root mean square error and maximum error are provided for both hearts, before and after annuloplasty. Annular dimensions, anteroposterior (AP) and transverse, as well as ring size (measured transversely) are provided in millimeters for reference.

				Pre-Annuloplasty		Post-Annuloplasty	
	AP	Transverse	Ring Size	E_{rms}	E_{max}	E_{rms}	E_{max}
Heart 1	18	22	18	0.55	1.67	0.63	1.84
Heart 2	16	26	20	0.67	1.81	0.75	1.96

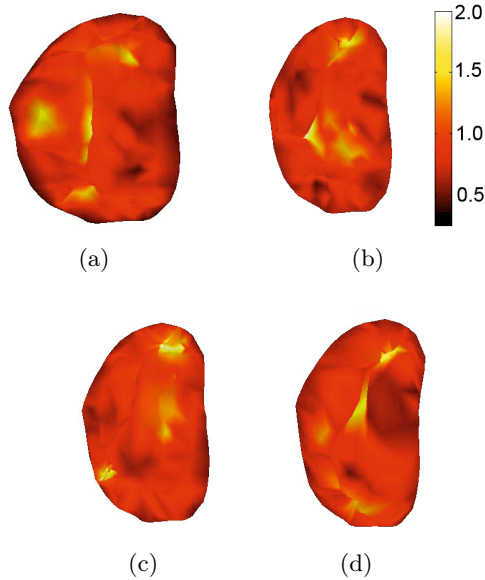


Fig. 2. Simulation error is mapped onto the simulated, closed valve shape of both hearts. Images (a) and (b) show the error before annuloplasty, while images (c) and (d) show the error after.

4 Discussion

The goal of this work was to progress the simulation of mitral annuloplasty towards clinical relevancy. To do so, simulation speed needed to be drastically increased without sacrificing accuracy. This required a series of model simplifications and design choices that reduced computational complexity. Validation is thus essential to determine accuracy following these simplifications.

The most significant of these reductions occurred through the loading of the valve. By electing to introduce a static load and only simulate the valve at a single state (namely under peak systolic load), the dynamics associated with the complex blood flow inside the left ventricle are not considered. However, choosing to simulate only peak systole can be justified on multiple grounds. From a practicality standpoint, it is currently infeasible to model the dynamic blood flow and produce a simulation that could run at sufficient speed to be clinically justifiable. From an information standpoint, static loading of the valve is already a test used intraoperatively to assess valve competency. Our work merely provides this information prior to the surgical modification of the valve, which is often difficult to reverse and is time-sensitive due to the use of cardiopulmonary bypass. Therefore, while we are not directly simulating the physiological process a valve undergoes during systole, we are simulating an approximation which has proven to be useful in practice allowing for informed decisions to be made preoperatively.

Nevertheless, even simulating this approximation would be too time-consuming to fit in a typical surgeon's workflow. Anything other than confirming the effectiveness of a single surgical plan would be difficult as there would be substantial delays between the input of a given procedure and the resulting closed valve shape. Ideally, the surgeon would be able to simulate multiple repair strategies, glean insights from previous attempts, to construct an optimal repair plan. To minimize simulation time and enable this iterative plan development, further efforts were made to decrease computational complexity. The implementation of a mass-spring tissue model in lieu of a finite element model reduced the complexity of tissue modeling by an order of magnitude. In addition, by downsampling the meshes to a lower resolution, a technique which has been shown to have minimal effect on the accuracy of valve models [17], computational burden was further reduced. Finally, simulation time is also aided by the sweep and prune broadphase collision detection algorithm, which exploits the temporal coherency in the simulation.

With these model simplifications and design decisions, root-mean-square error across the valves was 0.61 mm pre-annuloplasty, and 0.69 mm post-annuloplasty. Even though the annulus of the first heart was originally dilated (i.e., an anteroposterior-transverse ratio of near unity) and both rings were intentionally undersized to produce noticeable changes in valve geometry, simulation accuracy varied minimally after ring implantation. While this demonstrates accuracy was not compromised in achieving the sub-second simulation time, the benefit of having an accurate chordal structure must also be acknowledged. Typically, mitral valve simulations using image-based leaflet models implement a generic chordal geometry due to difficulties in ascertaining the geometry in-vivo [12]. However, the importance of an accurate chordal structure has already been demonstrated in [17]. While not particularly surprising given the known importance of the chordae amongst cardiac surgeons, it does further justify the use of microCT as a precise model of the chordae can be formed, minimizing geometric modeling error and thereby allowing for improved characterization of mechanical modeling error.

The use of microCT and non-physiological loading did have effects elsewhere in the study however. Preliminary specimens were treated with a different ring whose design was taken from a common complete planar ring. However, this ring consistently produced a small regurgitation along the posteromedial commissure. While such trace leaks are often insignificant intraoperatively, in this study they were significant. Regurgitation complicates pressure calculations as flow losses must be computed, and residual leaflet motion can produce ghosting in the images. This observed leak can largely be attributed to the original ring design. Rigid rings are developed with a contractile left ventricle in mind. In this study, with valve closure induced via pressurization rather than contraction of the left ventricle, ventricular dilation displaces the papillaries placing the heart in a non-physiological state. As a result, it is not surprising that an invasive ring designed for a contractile, regurgitant valve fails to ensure complete valve competency in a dilated, non-regurgitant valve. To combat this, modifications were made to the ring design to eliminate regurgitation, resulting in the final design shown in 1(b) which resembles the common Carpentier-Edwards Classic Annuloplasty Ring.

5 Conclusion

In this work, we have demonstrated it is feasible to use image-based models to quickly and accurately predict closed valve shape post-annuloplasty. In the future, the challenge will be to produce accurate geometric models in a non-destructive manner using clinical imaging modalities such as ultrasound or cardiac CT. While this would allow for in-vivo validation, it would also permit the clinical application of this technique, perhaps enabling the design and implementation of patient-specific rings.

References

1. Bonow, R.O., Carabello, B.A., Chatterjee, K., de Leon Jr., A.C., Faxon, D.P., Freed, M.D., Gaasch, W.H., Lytle, B.W., Nishimura, R.A., O’Gara, P.T., O’Rourke, R.A., Otto, C.M., Shah, P.M., Shanewise, J.S.: ACC/AHA 2006 guidelines for the management of patients with valvular heart disease. *Journal of the American College of Cardiology* 48, e1–e148 (2006)
2. Moss, R., Humphries, K., Gao, M., Thompson, C., Abel, J., Fradet, G., Munt, B.: Outcome of mitral valve repair or replacement: a comparison by propensity score analysis. *Circulation* 108(90101), II–90 (2003)
3. Gammie, J.S., Sheng, S., Griffith, B.P., Peterson, E.D., Rankin, J.S., O’Brien, S.M., Brown, J.M.: Trends in mitral valve surgery in the united states: Results from the society of thoracic surgeons adult cardiac database. *Annals of Thoracic Surgery* 87, 1431–1439 (2009)
4. Gillinov, A.M., Cosgrove, D.M., Blackstone, E.H., Diaz, R., Arnold, J.H., Lytle, B.W., Smedira, N.G., Sabik, J.F., McCarthy, P.M., Loop, F.D.: Durability of mitral valve repair for degenerative disease. *Journal of Thoracic and Cardiovascular Surgery* 116, 734–743 (1998)

5. Votta, E., Le, T.B., Stevanella, M., Fusini, L., Caiani, E.G., Redaelli, A., Sotiropoulos, F.: Toward patient-specific simulation of cardiac valves: State-of-the-art and future directions. *Journal of Biomechanics* 46, 217–228 (2013)
6. Votta, E., Maisano, F., Bolling, S.F., Alfieri, O., Montevicchi, F.M., Redaelli, A.: The geoforn disease-specific annuloplasty system: A finite element study. *Annals of Thoracic Surgery* 84, 92–102 (2007)
7. Kunzelman, K., Reimink, M., Cochran, R.: Flexible versus rigid ring annuloplasty for mitral valve annular dilation: A finite element analysis. *Journal of Heart Valve Disease* 7, 108–116 (1998)
8. Wenk, J., Zhang, Z., Cheng, G., Malhotra, D., Acevedo-Bolton, G., Burger, M., Suzuki, T., Saloner, D., Wallace, A., Guccione, J.: First Finite Element Model of the Left Ventricle With Mitral Valve: Insights Into Ischemic Mitral Regurgitation. *The Annals of Thoracic Surgery* 89(5), 1546–1553 (2010)
9. Bothe, W., Rausch, M.K., Kvitting, J.-P.E., Echnner, D.K., Walther, M., Ingels Jr., N.B., Kuhl, E., Miller, D.C.: How do annuloplasty rings affect mitral annular strains in the normal beating ovine heart? *Circulation* 126, S231–S238 (2012)
10. Bothe, W., Kuhl, E., Kvitting, J.P.E., Rausch, M.K., Goktepe, S., Swanson, J.C., Farahmandnia, S., Ingels Jr., N.B., Miller, D.C.: Rigid, complete annuloplasty ring increase anterior mitral leaflet strains in the normal beating ovine heart. *Circulation* 124, S81–S96 (2011)
11. Hammer, P., Vasilyev, N., Perrin, D., Del Nido, P., Howe, R.: Fast image-based model of mitral valve closure for surgical planning. In: *MIDAS Journal, Computational Biomechanics for Medicine (MICCAI 2008 Workshop)*, pp. 15–26 (2008)
12. Voigt, I., Ionasec, R.I., Georgescu, B., Houle, H., Huber, M., Hornegger, J., Comaniciu, D.: Model-driven physiological assessment of the mitral valve from 4d tee. In: *Proceedings of Society of Photo-Optical Instrumentation Engineers* (2009)
13. Schneider, R.J., Tenenholtz, N.A., Perrin, D.P., Marx, G.R., del Nido, P.J., Howe, R.D.: Patient-specific mitral leaflet segmentation from 4D ultrasound. In: Fichtinger, G., Martel, A., Peters, T. (eds.) *MICCAI 2011, Part III. LNCS*, vol. 6893, pp. 520–527. Springer, Heidelberg (2011)
14. Hammer, P., Sacks, M., del Nido, P., Howe, R.: Mass-spring model for simulation of heart valve tissue for mechanical behavior. *Annals of Biomedical Engineering* 39, 1668–1679 (2011)
15. May-Newman, K., Yin, F.: Biaxial mechanical behavior of excised porcine mitral valve leaflets. *American Journal of Physiology-Heart and Circulatory Physiology* 269(4), H1319 (1995)
16. Tenenholtz, N.A., Hammer, P.E., Schneider, R.J., Vasilyev, N.V., Howe, R.D.: On the design of an interactive, patient-specific surgical simulator for mitral valve repair. In: *2011 IEEE/RSJ International Conference on Intelligent Robots and Systems (IROS)*, pp. 1327–1332. IEEE (2011)
17. Hammer, P.E., del Nido, P.J., Howe, R.D.: Anisotropic mass-spring method accurately simulates mitral valve closure from image-based models. In: Metaxas, D.N., Axel, L. (eds.) *FIMH 2011. LNCS*, vol. 6666, pp. 233–240. Springer, Heidelberg (2011)